Macromolecular Journals

Macromolecular Materials and Engineering

Miscibility and Phase Morphology of MF/PVAc Hybrid Resins for Surface Bonding of Building Interior Materials

Sumin Kim, Hyun-Joong Kim*

The objective of this research was to investigate the miscibility behavior of melamine-formaldehyde resin and poly(vinyl acetate) blends for use as adhesives for surface materials in order to reduce formaldehyde emission. The investigation was conducted using differential scanning calorimetry, Fourier transform infrared spectroscopy, ^{13}C CP/MAS solid state NMR, scanning electron microscope, atomic force microscopy and wide-angle X-ray scattering. Blends of various MF resin/PVAc weight compositions, comprising 0, 30, 50, 70 and 100%, were prepared in order to determine and compare the effect of PVAc content. These blends displayed a single cure temperature over the entire range of compositions indicating that this blend system was miscible in the amorphous phase due to the formation of hydrogen bonding between the amine groups of the MF resin and the carbonyl groups of PVAc. On the surface of the cured blends, the homogeneous dispersion of the PVAc phase in the MF resin was evident as small spherical domains and the blends were confirmed to be well combined.

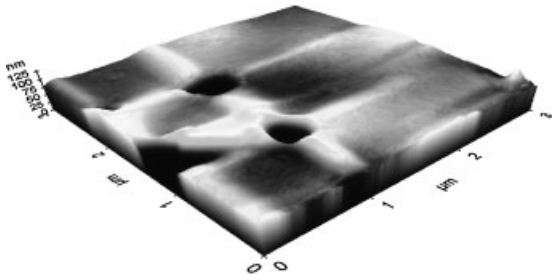

Introduction

Thermosetting polymers are among the most important materials in many industries and are becoming increasingly used in engineering applications. They are generally amorphous, highly-crosslinked polymers, possessing various excellent properties such as high tensile strength and modulus, easy processing, good thermal and chemical resistance and dimensional stability. However, they have low toughness and poor crack resistance, and are hence normally brittle at room temperature. Nevertheless, relatively few systematic studies have investigated the miscibility, phase behavior and morphology in blends of thermosetting resins with linear polymers.[1–11] The resulting morphology and extent of phase separation is known to affect the final optical and mechanical properties of the cured blends. Therefore, there is great practical importance in developing an understanding of the miscibility, phase behavior and morphology in thermosetting polymer blends. Furthermore, much academic interest has focused on examining these basic aspects of thermosetting polymer blend systems. The interrelationship between the miscibility, phase behavior, morphology and composition in thermosetting polymer blends is complicated and can be remarkably affected by cross-linking.[12] These days, melamine-formaldehyde (MF) and

S. Kim, H.-J. Kim
Laboratory of Adhesion & Bio-Composites, Program in Environmental Materials Science, Seoul National University, Seoul 151-921, South Korea
Fax: +82-2-873-2318; E-mail: hjokim@snu.ac.kr

DOI: 10.1002/mame.200600354

melamine-urea-formaldehyde (MUF) resins are mainly used as thermosetting wood adhesives for wood-based panels. Both resins give excellent adhesive performance, good moisture resistance and also tend to produce lower formaldehyde emissions than urea-formaldehyde resins. Recently, the finding that MUF resin hardening occurs mostly due to its melamine reactivity has led to the realization that the development of a mechanism or system of hardening, in order to improve the performance or to lower the formaldehyde emissions of MF, can be more easily obtained with pure MF resins than with MUF resins.[13,14]

Interest in poly(vinyl acetate) (PVAc)-based materials having higher bond strength and better film properties has grown considerably in the past two decades in the adhesive, paint, paper and textile industries.[15] Its application is very easy and it does not damage the tools during the cutting process. However, the mechanical resistance of PVAc adhesive decreases with increasing temperature and it loses its bonding capacity above 70 °C.[16,17] When PVAc was added to MF resin and the resulting blend was used to bond plywood and fancy veneer in engineered flooring, the formaldehyde emission was dramatically reduced.[18]

Huang et al. studied the miscibility of thermo-setting resins and PVAc blends.[19] It was found that the phenolic/PVAc blends were miscible in the amorphous phase over the entire composition range. The results obtained by differential scanning calorimetry (DSC), Fourier transform infrared (FT-IR) spectroscopy and high-resolution solid-state ^{13}C NMR revealed strong inter-association hydrogen bonds between the hydroxyl groups of phenolic and the carbonyl groups of PVAc.[19] In the case of blends of phenolic resin with polymers such as poly(ethylene vinyl acetate) and aliphatic polyester, it was reported that hydrogen bond formation was critical in enhancing the miscibility of the various phenolic blends with modifiers containing ether, carbonyl, or hydroxyl functional groups.[20,21] Considerable effort has been made to study the miscibility and phase behavior of different polymer blends.[22] Intermolecular interactions are usually considered to be the driving force for miscibility, and their important role in the miscibility of polymer blends has been clearly demonstrated.[23]

To understand the behavior of these polymer blends, it is necessary to characterize the interaction of the components. There are several techniques that can be used to inveterate polymer blends' interactions at different scales, two of which are SEM and NMR.[24]^{13}C solid-state NMR has proven to be a very useful method for investigating not only the molecular motion but also the scale of miscibility.[25] It is a powerful technique that has been utilized in analyzing miscibility, phase structure and heterogeneity in polymer mixtures on a molecular scale.[26–30]

The performance of the polymer material can be efficiently improved by combining existing polymers in a suitable way. It has been shown that the properties of polymer blends, including strength and toughness, have close relations with their internal microscopic phase morphology.[31–33] Moreover, the formation and evolution of the phase morphology strongly depend on the melt mixing process. Thus, the dynamics during melt mixing have a large effect on the macroscopic properties of the blends, as has been reported in many works.[34–36] The microscopic phase morphology of polymer alloys can be directly observed by some microscopy methods such as SEM and TEM. The SEM patterns provide information on some of the physical parameters, such as component concentration and orientation, in the space. As a matter of fact, the pattern formation and selection are equivalent to the formation and controlling of the phase morphology in polymer material science.[37]

In this study, MF resin was blended with PVAc, the miscibility and crystallization of the resulting polymers were studied by a variety of techniques including FT-IR, DSC and solid state ^{13}C NMR. Additionally, this study was focused on the effect of various composition ratios on the phase behavior and morphology as determined by SEM and AFM.

Experimental Part

Materials

The MF resin was synthesized in the laboratory. The resin was prepared at an F/M molar ratio of 1.75, with a solid content of 49 wt.-%. After the addition of water to the formalin, to 38.5 wt.-% formaldehyde in water, the pH was adjusted to 9.0 by adding a 1 M NaOH solution (because the methylolated intermediates of the reaction rapidly condense under acidic conditions) and the melamine was added. As hardener, 10% NH_4Cl solution was used. The viscosity as measured using a Brookfield Viscometer Model DV-II+ was 140 cP at 21 °C. PVAc in liquid form was used with a density of 1.1 $g \cdot cm^{-3}$, viscosity of 2 000 cP at 21 °C, pH of 5 and ash ratio of 3%. PVAc adhesive was supplied from Tae Yang Chemical Co. Ltd (Incheon, Korea).

Blend Preparations

Blends with various compositions of MF resin/PVAc content ratios were prepared. To determine and compare the effect of PVAc content, compositions of 0, 30, 50, 70 and 100 wt.-% of MF resin, were used. The blends were merely mixed by stirring and all were 5-blending systems.

Differential Scanning Calorimetry (DSC)

The T_g of the blends was determined by a DSC with TA Instrument Q-1000, with a scan rate of 10 °C · min^{-1} over a temperature range

Macromol. Mater. Eng. 2007, 292, 339–346

Macromolecular Journals

DOI: 10.1002/mame.200600354

of −50 to 100 °C. The measurement was made using a 5–10 mg sample on a DSC sample cell after the sample was quickly cooled to −50 °C from the melt of the first scan. The T_g was taken as the midpoint of the heat capacity transition between the upper and lower points of deviation from the extrapolated liquid and glass lines. A sealed liquid type, aluminum capsule pan was used, under a nitrogen atmosphere.

FTIR-ATR Spectroscopy

FTIR-ATR spectra were recorded on a Nicolet Magna 550 Series II spectrometer at a resolution of 4 cm^{-1}, in the mid-infrared range from 4 000 to 600 cm^{-1} in the absorbance mode for resin characterization during the curing process. To enhance the signal-to-noise ratio, each of the reference and sample spectra represents the average of 40 scans recorded at 4 cm^{-1} resolution. The temperature and relative humidity of the FTIR spectroscopic analysis samples were 23 ± 1 °C and 60%, respectively. Samples for spectroscopic analysis were obtained by the solvent casting method. Crystallization from the melt was performed by holding the sample for 3 min at 150 °C in order to cure. The surfaces of the analyzed samples were in contact with a ZnSe crystal with a 45 ° angle of incidence. Net peak heights were determined by subtracting the height of the baseline immediately before the peak from the total peak height.

Solid State NMR

High-resolution, solid-state NMR experiments were carried out on a Bruker DSX-400 spectrometer operating at resonance frequencies of 399.53 and 100.47 MHz for ^1H and ^{13}C, respectively. The ^{13}C CP/MAS spectra were measured with a 3.9 μs 90 ° pulse, 3 s pulse delay time, and 30 ms acquisition time, while 2 048 scans were accumulated. All NMR spectra were taken at 300 K using broad band proton decoupling and a normal cross-polarization pulse sequence. A magic angle sample-spinning (MAS) rate of 5.4 Hz was used to eliminate resonance broadening due to the anisotropy of chemical shift tensors. The proton spin-lattice relaxation time in the rotating frame ($T_{1\rho}^{H}$) was measured indirectly via carbon observation using a 90 °-τ-spin lock pulse sequence prior to cross-polarization. The data acquisition was performed via ^1H decoupling and delay time (τ) ranging from 0.3 to 15 ms with a contact time of 1.0 ms.

SEM

The surfaces of the cured MF/PVAc hybrid resins underwent analysis using a SIRIOM SEM (FEI Co.) from the U.S.A. In addition, a SEM equipped with EDX elemental composition analyzer was used to analyze all blend systems. All samples were cured in a dry oven at 60 °C for 2 h. The acceleration potential used during this investigation was 20 kV. Total scanning time during elemental map generation was 20 min. Prior to the measurement, the specimens were coated with gold (purity, 99.99%) to eliminate electron charging.

AFM

Surface topology images of MF/PVAc hybrid resins immobilized on the two types of base layer were acquired using an atomic force microscope (AFM, XE-100, PSIA, Korea) operated in non-contact mode. The average surface roughness (R_a) for each AFM image was calculated by means of the software provided with the instrument. AFM images were obtained using non-contact mode in which the cantilever tip hovers about 50–150 Å above the sample surface to detect the attractive van der Waals forces acting between the tip and the sample. Topographic images are constructed by scanning the tip above the surface. The scan size and scan speed were 3 μm and 0.3 Hz, respectively.

X-Ray Analysis

Wide-angle X-ray scattering (WAXS) analysis of MF resin, PVAc and the blends was performed with a Bruker General Area Detector Diffraction System (GADDS; NICEM at Seoul National University) that recorded the intensity of the X-rays diffracted by the sample as a function of the Bragg angle using Bruker computer software. CuK_α radiation with wavelength $\lambda = 1.54$Å was used with a nickel filter. The exposure time was 300 s with a 0.02 ° (2θ) step. Two dimensional scattering patterns were obtained by means of a Hi-Star X-ray detector.

Results and Discussion

DSC

Thermal characterization of polymer blends is a well-known method for determining their miscibility. The miscibility between any two polymers in the amorphous state is evidenced by the presence of a single T_g.[19,38] The DSC curves of the MF resin/PVAc blends are shown in Figure 1. It can be seen that, each blend displayed a single T_g, intermediate between those of the two pure components and varying with the blend composition. Therefore, it was judged that MF resin/PVAc blends are completely miscible over the entire composition range. In particular, the T_g of the blends was dependent on the blend composition, confirming the miscibility of the PLA/PVA system over the entire composition range. In general, blend miscibility is often quantified by analyzing its dependence on composition. Traditionally, equations based on the free volume hypothesis have been used to model the composition dependence of T_g. They are expressed as the Fox[39] and Gordon-Taylor[40] equations. The Fox equation is:

$$\frac{1}{T_g} = \frac{W_1}{T_{g1}} + \frac{W_2}{T_{g2}} \quad (1)$$

where W_i is the weight fraction of component i, T_g the blend T_g and T_{gi} the T_g of neat component i. This equation

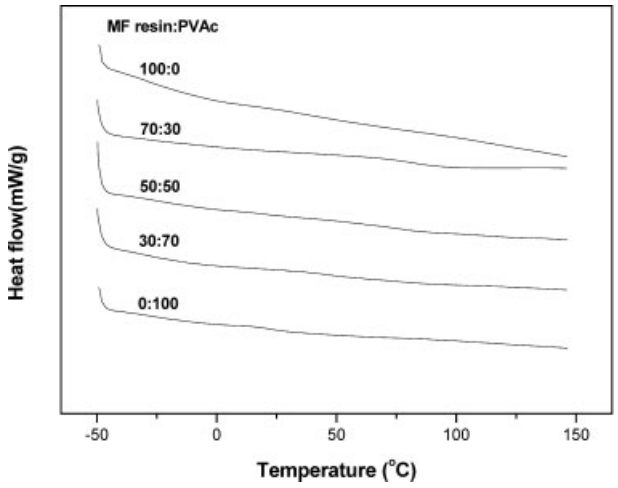

Figure 1. DSC scans of MF resin/PVAc blends with different compositions: 100/0, 70/30, 50/50, 30/70 and 0/100.

assumes that the specific heats of the two components are identical. The Gordon–Taylor equation is:

$$T_g = \frac{W_1 T_{g1} + kW_2 T_{g2}}{W_1 + kW_2} \quad (2)$$

where the G-T parameter k is formally equal to $\Delta\alpha_2/\Delta\alpha_1$, and $\Delta\alpha$ is the difference in the thermal expansion coefficient between the liquid and glassy states at T_{gi}. Generally, k is often used as a fitting parameter. In Figure 2, the curves calculated by the Fox and Gordon-Taylor equations are represented by the solid and dotted lines, respectively, which were obtained with a value of $k = 2.8$. Gajria et al.[41] have reported that the T_g curve with various blend compositions was in good agreement with the values calculated by the Fox equation. However, in our work, the observed values were consistent with those calculated by the Gordon-Taylor equation using a value of $k = 2.8$ rather than those by the Fox equation. Huang et al.[19] reported that the parameter q in the Kwei equation[42] corresponds to the strength of hydrogen bonding in the blend and that a relatively large value for q reflects a strong intermolecular interaction between MF resin and PVAc.

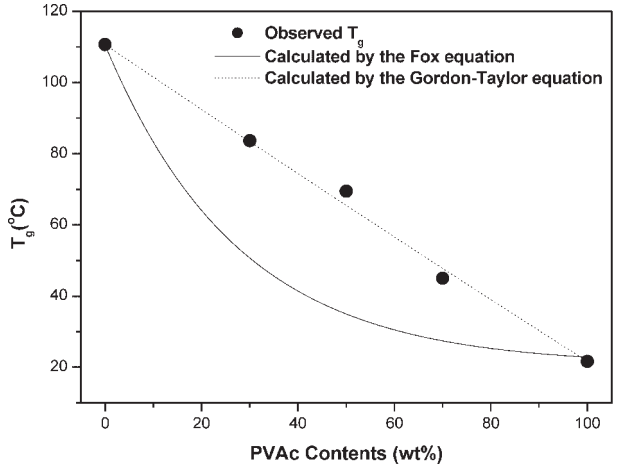

Figure 2. Variation of glass transition temperature with blend composition.

FT-IR

FT-IR is a particularly suitable method to determinate the presence of specific interactions between various groups in polymer blends due to the force constants, and it is sensitive to both inter- and intra-molecular interactions.[19] In order to obtain more information on the miscibility, the crystallization behavior of MF resin in the blend system was studied by FT-IR spectroscopic measurements. Figure 3 presents the FT-IR spectra of MF resin, PVAc and their blends solvent-cast at room temperature and cured for 3 min at 150 °C. The signal at 1 733 cm^{-1} is characteristic of the carbonyl (C=O) stretching of the PVAc. This peak increased with increasing PVAc addition ratio. The carbonyl absorption peak was located at approximately 1 733 cm^{-1} for all compositions and the peak shift was negligible. The lack of peak shifting suggests that a relatively low level of specific interactions, if any, was present between the two molecules. Additionally, the carbonyl group of PVAc might not have interacted specifically with any specific sites of the MF resin molecule. The deformation peak for the MF resin, which can be conveniently compared, gave absorption bands in the 1 546–1 558 cm^{-1} range, the 1 357–1 373 cm^{-1} range and the 1 006–1 022 cm^{-1} range.

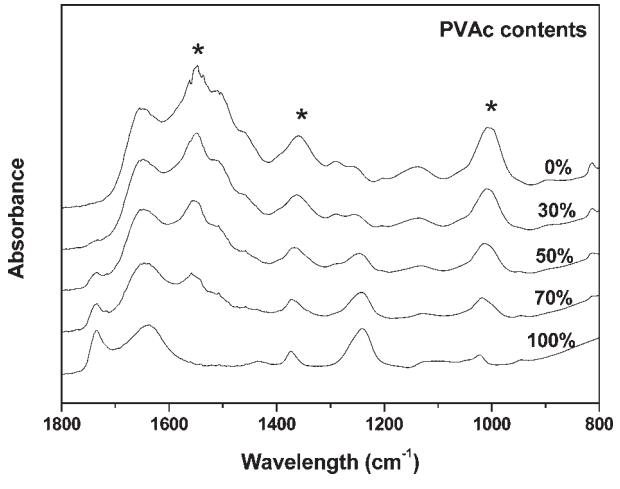

Figure 3. FT-IR spectra at 25 °C in the 800–1 800 cm^{-1} region for MF resin/PVAc blends cured for 3 min at 150 °C: 100/0, 70/30, 50/50, 30/70 and 0/100.

Macromol. Mater. Eng. **2007**, *292*, 339–346

Macromolecular Journals

DOI: 10.1002/mame.200600354

As these three bands were sensitive to the degree of crystallinity, we were particularly interested in them. As shown in Figure 3, the band intensity at these bands decreased with increasing PVAc fraction, which is consistent with the fact that the degree of crystallinity of the MF resin decreased with increasing PVAc content. The degree of crystallinity by DSC was calculated from Equation (3):

$$Xc = \frac{\Delta H(\text{blend})}{\Delta H(\text{MF})} \quad (3)$$

where ΔH(blend) is the apparent enthalpy of fusion per gram of blend and ΔH(MF) is the thermodynamic enthalpy of fusion per gram of MF resin. The changes in the degree of crystallinity could be calculated in the FT-IR experiments by comparing the relative intensity of the band at 1 546–1 558 cm^{-1}, which displayed the largest difference in intensity between the crystalline and amorphous states and was better resolved than the other two crystallinity-sensitive bands at 1 357–1 373 and 1 006–1 022 cm^{-1}. The degree of crystallinity was obtained by normalizing the absorbance at 900 cm^{-1} to that of the 1 800 cm^{-1} band. Hence, a crystallinity index (CI) was defined as the ratio of the intensities of the band at 900 cm^{-1} to that at 1 800 cm^{-1}. This crystallinity index should not be confused with the absolute degree of crystallinity. Figure 4 shows the changes in the degree of crystallinity observed by FT-IR and DSC measurements. It is shown that the crystallinity index measured by FT-IR of MF resin decreased with increasing PVAc content. This behavior agrees with the DSC studies, in which the same trend was observed for blend samples.

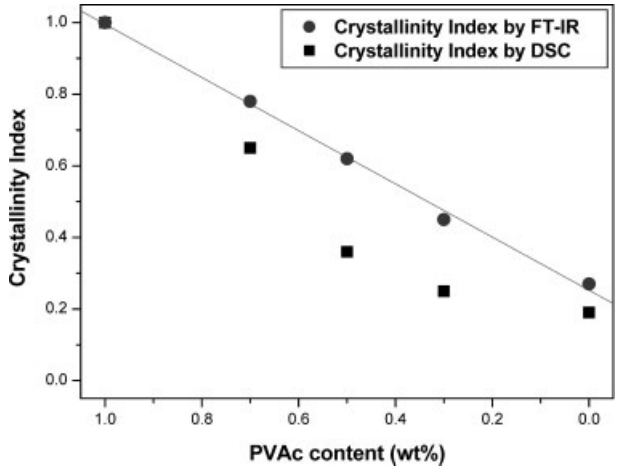

Figure 4. Crystallinity index (CI) of MF resin/PVAc blends from FT-IR and DSC measurements.

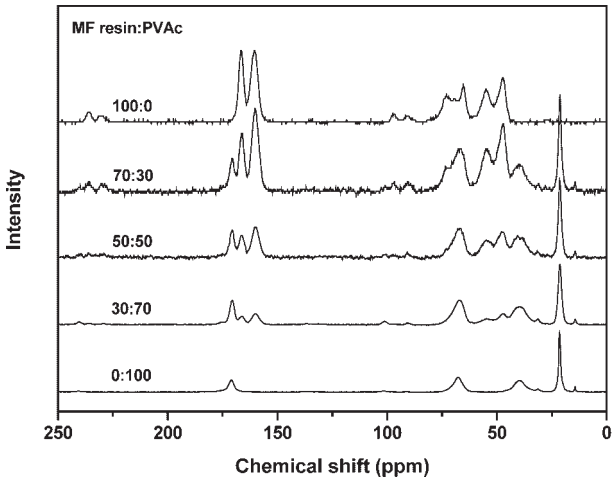

Figure 5. ^{13}C CP/MAS spectra of MF resin/PVAc blends cured for 3 min at 150 °C: 100/0, 70/30, 50/50, 30/70 and 0/100.

NMR

Figure 5 shows the ^{13}C CP/MAS NMR spectra of MF resin, PVAc and the MF/PVAc blends. Assignments of molecular groups to the spectra are shown in Table 1, and are in accord with assignments previously reported in the literature.[43–48] The ^{13}C CP/MAS spectrum with dipolar dephasing was recorded. Four signals were detected as PVAc peaks, and one at 171.2 ppm referred to a C=O of carboxyl group. This peak increased with increasing PVAc addition ratio. The carbonyl absorption peak was located at approximately 171.2 ppm for all compositions and the peak shift was negligible. The lack of peak shifting suggests that the specific interactions between the two molecules were relatively low, if present at all. Additionally, the carbonyl group of PVAc might not have interacted

Table 1. Assignments of molecular groups to the ^{13}C CPMAS spectra of MF resin and PVAc. All other peaks in the spectra were spinning side bands.

Resin	Chemical shift	Assignment
	ppm	
PVAc	21.4	CH_3–C=O
	39.8	>CH–CH_2–CH<
	67.5	–O=C–O–CH<
	171.2	–C=O
MF resin	47.2	–NHCH_2NH–
	54.5	–N(CH_2–)CH_2NH–
	65.3	–NHCH_2OH
	72.6	–N(CH_2–)CH_2OH
	160.4	>NCON<
	166.4	–N=C(NH_2)–N=

specifically with any specific sites of the MF resin molecule. A second peak at 39.8 ppm was attributed to the CH_2 group, but the signal was inverted due to the absence of complete dephasing. The last peak at 21.4 ppm was attributed to the methyl group. Although carbon-13, which has rapid rotation even in solids, $^{13}C-^{1}H$ dipolar interactions, as well as non protonated carbons, are expected to be observed. The methyl and CH–O groups have high mobility. The deformation of the peak for the MF resin, which can be conveniently compared, gave peaks at 47.2, 54.5, 5.3, 72.6, 160.4 and 166.4 ppm.

The chemical shift of the carbonyl carbon of the PVAc increased with increasing MF resin content. A downfield shift of 3 ppm was observed in the MF resin/PVAc 70:30 blend relative to the pure PVAc. It is well known that the existence of specific interactions in polymer blends will affect the chemical environment of the neighboring molecules, cause changes of magnetic shielding and, therefore, move the chemical shift downfield.[19] A similar chemical shift was also observed for the hydroxyl-substituted carbon of MF resin, which was shifted downfield with increasing PVAc content. A downfield shift of 2.5 ppm was observed in the MF resin/PVAc 30:70 blend relative to the pure amine, indicating intermolecular hydrogen bonding between the amine group of MF resin and the carbonyl group of PVAc. These results are consistent with the previous FT-IR results.

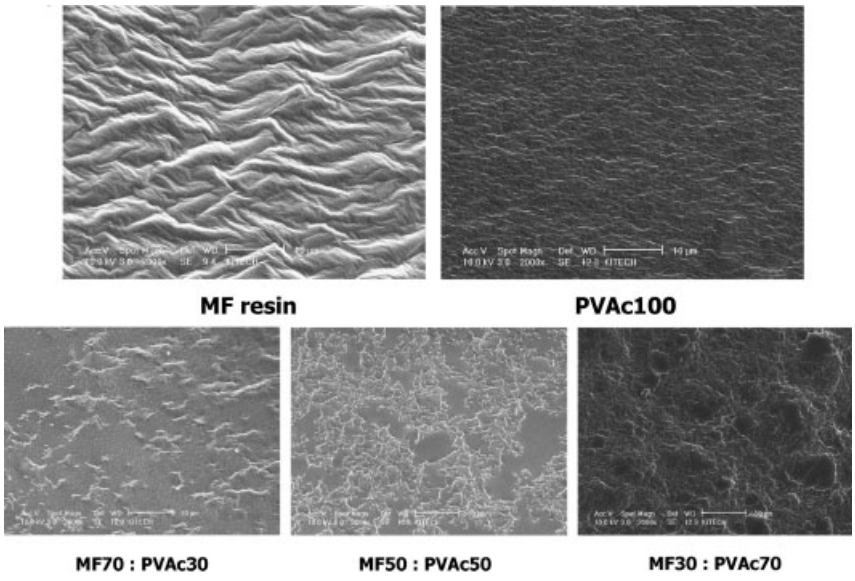

Figure 6. SEM photographs of MF resin/PVAc blends cured for 1 h at 120 °C: 100/0, 70/30, 50/50, 30/70 and 0/100.

spherical domains. This tendency was also shown in the AFM topographic images of Figure 7. For the MF resin/PVAc 70:30 blend, it can be seen that the spherical particles were uniformly dispersed in the continuous matrix. The spherical phase was attributed to the PVAc-rich phase whereas the continuous phase was ascribed to the MF resin matrix. With increasing PVAc content, the blends displayed remarkably different morphologies. For the MF resin/PVAc 70:30 blend, the PVAc domains began to inter-connect and exhibited irregular shapes. At the same time, spherical particles appeared on the surface of the

Morphology

The morphology of the MF resin, PVAc and blends was investigated by SEM and AFM. SEM micrographs of the surfaces of cured MF resin, PVAc and blends are shown in Figure 6. A heterogeneous morphology was observed in all the cases, which was in a good agreement with the DSC results; that is, the blends were well combined. The MF resin matrix presented small cavities, which confirms that PVAc was homogeneously dispersed in the MF resin matrix. From this figure, a very fine and homogeneous dispersion of the PVAc phase in the MF resin can be seen as small

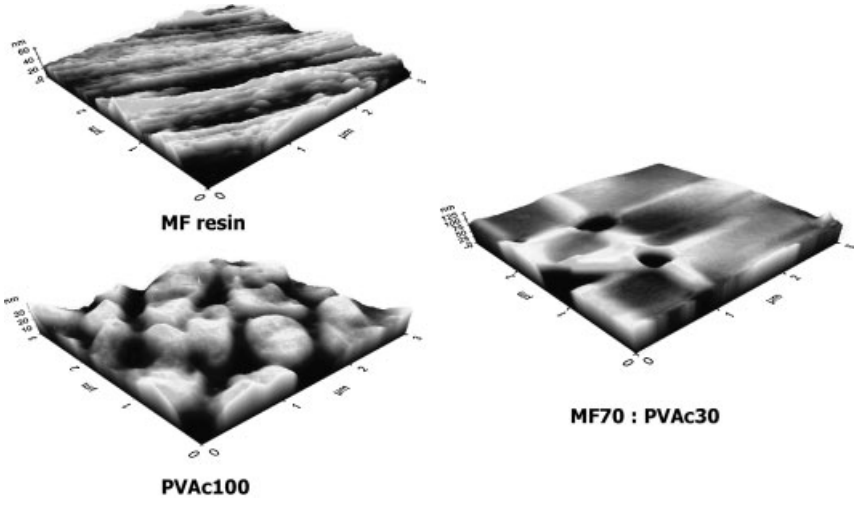

Figure 7. AFM images of MF resin/PVAc blends cured for 1 h at 120 °C: 100/0, 70/30 and 0/100.

DOI: 10.1002/mame.200600354

etched blends with a broad size distribution, and which were responsible for the MF resin phase. This was therefore demonstrated to be a combined morphology; that is, phase inversion began to appear. A totally phase-inverted morphology was observed for blends with PVAc content more than 30 wt.-%. However, in the case of PVAc 30 wt.-%, the morphology was similar to that of PVAc only. Like the peak shifts in FT-IR and ^{13}C CP/MAS NMR, the blend morphologies were shifted to each typical morphology, as shown in the AFM topographic images of Figure 7.

Wide-Angle X-Ray Scattering

In the WAXS diffraction curves of PVAc, two peaks at angles $2\theta = 3.7$ and 21.55 ° were superimposed on a widely diffused peak distribution of diffracted X-rays by reflection mode, as shown in Figure 8. MF resin showed strong diffraction peaks at 2θ of 13.4 and 21.28 °. The MF/PVAc 50:50 blend is shown in the middle of the two peaks. The peaks of 3.7 and 21.55 ° decreased while that of 13.4 ° increased with an increasing proportion of PVAc in the blends. The WAXS results in this study indicated that any change of crystal and amorphous structure between the functional groups in the MF resin and PVAc was likely to be low or non-specific. These results showed a similar tendency as the peak changes of FT-IR and ^{13}C CP/MAS NMR.

Conclusion

MF resin and PVAc were blended at varying ratios to reduce the formaldehyde emission from surface materials. We investigated the miscibility behavior between the MF resin and PVAc to obtain optimum adhesion. Thermal analysis showed that all blends displayed a single cure peak temperature (T_c), which was intermediate between those of the two pure components and which varied with the blend composition. FT-IR results showed that the characteristic peaks of the MF resin (amine) and PVAc (carboxyl) changed regularly over the range of blend ratios from 0 to 100%. The MF resin/PVAc blends were miscible in the amorphous phase over the entire composition range. The observed values were consistent with those calculated by the Gordon-Taylor equation using a value of $k = 2.8$, rather than with those by the Fox equation. In the ^{13}C CP/MAS NMR spectra results, the chemical shift of the carbonyl carbon of the PVAc increased with increasing MF resin content. A downfield shift of 2.5 ppm was observed in the MF resin/PVAc 30:70 blend relative to that of pure amine, indicating intermolecular hydrogen bonding between the amine group of MF resin and the carbonyl group of PVAc. At the surface of the cured blends, a homogeneous dispersion of the PVAc phase in the MF resin was evident as small spherical domains, indicating the good combination of the blends.

Acknowledgements: This work was financially supported by the *Seoul R. & B. D.* program. Sumin Kim is grateful for the graduate fellowship provided by the *Ministry of Education* through the *Brain Korea 21* project.

Received: September 20, 2006; Revised: November 21, 2006; Accepted: November 28, 2006; DOI: 10.1002/mame.200600354

Keywords: blends; hydrogen bonding; melamine-formaldehyde (MF) resin; miscibility; morphology; poly(vinyl acetate) PVAc

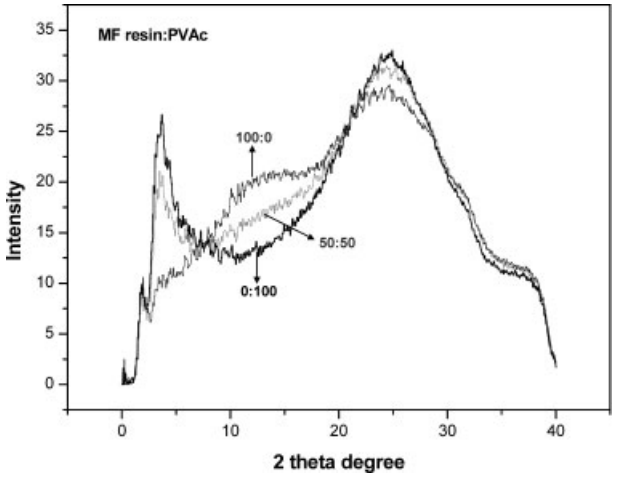

Figure 8. WAXS diffraction curves of MF resin/PVAc blends cured for 1 h at 120 °C: 100/0, 50/50 and 0/100.

[1] Q. Guo, *Polymer Blends and Alloys*, Vol. 6, G. O. Shonaike, G. Simon, Eds., Marcel Dekker, New York 1999, p. 155.
[2] T. Inoue, *Prog. Polym. Sci.* **1995**, *20,* 119.
[3] Q. Guo, X. Peng, Z. Wang, *Polymer* **1991**, *32,* 53.
[4] H. Zheng, S. Zheng, Q. Guo, *J. Polym. Sci. Polym. Chem. Ed.* **1997**, *35,* 3161.
[5] Z. Zhong, Q. Guo, *Polymer* **1998**, *39,* 517.
[6] M. A. Hillmyer, P. M. Lipic, D. A. Hajduk, K. Almdal, F. S. Bates, *J. Am. Chem. Soc.* **1997**, *119,* 2749.
[7] P. M. Lipic, F. S. Bates, M. A. Hillmyer, *J. Am. Chem. Soc.* **1998**, *120,* 8963.
[8] T. J. Horng, E. M. Woo, *Polymer* **1998**, *39,* 4115.
[9] J. L. Cheng, F. C. Chang, *Macromolecules* **1999**, *32,* 5348.
[10] J. Mijovic, M. Shen, J. W. Sy, *Macromolecules* **2000**, *33,* 5235.
[11] Q. Guo, C. Harrats, G. Groeninckx, M. H. J. Koch, *Polymer* **2001**, *42,* 4127.
[12] Q. Guo, P. Figueiredo, R. Thomann, W. Gronski, *Polymer* **2001**, *42,* 10101.
[13] S. Kim, H.-J. Kim, *J. Adhes. Sci. Technol.* **2006**, *20,* 705.
[14] A. H. Conner, *"Polymeric Materials Encyclopedia"*, J. C. Salamone, Eds., CRC Press, Boca Raton, FL 1996, p. 8496.

[15] S. K. Verma, S. C. Bisarya, *J. Appl. Polym. Sci.* **1986**, *31,* 2675.
[16] M. Dunky, *Int. J. Adhes. Adhes.* **1998**, *18,* 95.
[17] Ö. Yalçin, A. Musa, Ö. Ayhan, *J. Appl. Polym. Sci.* **2000**, *76,* 1472.
[18] S. Kim, H.-J. Kim, *Int. J. Adhes. Adhes.* **2005**, *25,* 456.
[19] M.-W. Huang, S.-W. Kuo, H.-D. Wu, F.-C. Chang, S.-Y. Fang, *Polymer* **2000**, *41,* 2479.
[20] N. Mekhilef, P. Hadjiandreou, *Polymer* **1995**, *36,* 2165.
[21] C.-C. M. Ma, H.-D. Wu, P. P. Chu, H.-T. Tseng, *Macromolecules* **1997**, *30,* 5443.
[22] L. A. Utracki, "*Polymer Alloys and Blends*", Hanser, Munich 1989.
[23] E. E. Shafee, *Polymer* **2002**, *43,* 921.
[24] C. M. G. Souza, M. I. B. Tavares, *J. Appl. Polym. Sci.* **1999**, *74,* 2990.
[25] J. Wanga, M. K. Cheung, Y. Mi, *Polymer* **2001**, *42,* 3087.
[26] E. O. Stejskal, J. Schaefer, M. D. Sefcik, R. A. McKay, *Macromolecules* **1981**, *14,* 275.
[27] L. C. Dickinson, H. Yang, C.-W. Chu, R. S. Stein, J. C. Chien, *Macromolecules* **1987**, *20,* 1757.
[28] K. Schmidt-Rohr, H. W. Spiess, "*Multidimensional Solid-State NMR and Polymers*", Academic Press, New York 1994.
[29] T. Yu, M. Guo, *Prog. Polym. Sci.* **1990**, *15,* 825.
[30] R.-R. Wu, H.-M. Kao, J.-C. Chiang, E. M. Woo, *Polymer* **2002**, *43,* 171.
[31] Y. Kayano, H. Keskkula, D. R. Paul, *Polymer* **1997**, *38,* 1885.
[32] L. Corté, F. Beaume, L. Leibler, *Polymer* **2005**, *46,* 2748.
[33] L. Corté, L. Leibler, *Fluid Phase Equilibr.* **2005**, *234,* 6360.
[34] C. E. Scott, C. W. Macosko, *Polymer* **1995**, *36,* 461.
[35] H. E. Burch, C. E. Scott, *Polymer* **2001**, *42,* 7313.
[36] S. C. Jana, M. Sau, *Polymer* **2004**, *45,* 1665.
[37] L.-T. Yan, J. Sheng, *Polymer* **2006**, *47,* 2894.
[38] S. Kim, H.-J. Kim, *J. Adhes. Sci. Technol.* **2006**, *20,* 209.
[39] T. G. Fox, *Bull. Am. Phys. Soc.* **1956**, *1,* 123.
[40] M. Gordon, J. S. Taylor, *J. Appl. Chem.* **1952**, *2,* 493.
[41] A. M. Gajria, V. Davé, R. A. Gross, S. P. McCarthy, *Polymer* **1996**, *37,* 437.
[42] T. K. Kwei, *J. Polym. Sci. Polym. Let. Ed.* **1984**, *22,* 307.
[43] D. J. Hill, M. Markotsis, A. K. Whittaker, K. W. Wong, *Polym. Int.* **2003**, *52,* 1780.
[44] C. M. G. Souza, M. I. B. Tavares, *J. Appl. Polym. Sci.* **2002**, *86,* 116.
[45] A. S. Angelatos, M. I. Burgar, N. Dunlop, F. Separovic, *J. Appl. Polym. Sci.* **2004**, *91,* 3504.
[46] A. T. Mercer, A. Pizzi, *J. Appl. Polym. Sci.* **1996**, *61,* 1687.
[47] A. T. Mercer, A. Pizzi, *J. Appl. Polym. Sci.* **1996**, *61,* 1697.
[48] L. A. Panangama, A. Pizzi, *J. Appl. Polym. Sci.* **1996**, *59,* 2055.

DOI: 10.1002/mame.200600354